


Reflection of light as a mechanical phenomenon applied to the Michelson interferometer with light from the Sun

January 11, 2023

Filip Dambi Filipescu 
filipdambi1@gmail.com

Abstract: The Sun is a frame at relative rest where its light travels at the emitted speed c . Earth travels at the revolving speed v in this frame. The reflection of light as a mechanical phenomenon applies to the modified Michelson interferometer employed by Miller in his experiments with light from the Sun. Unlike the Tomaschek experiments, which use light from stars that may travel in the Universe at velocities different from that of the Sun, the fringe shifts in the Miller experiments are predictable. Based on Michelson's derivation, Miller expected in his experiments at Mount Wilson a 1.12 fringe shift and observed a fringe shift of 0.08 in 1921 and 0.088 in 1925. The reflection of light as a mechanical phenomenon predicts zero fringe shift for Miller's experiment agreeing only with his observations at the Cleveland laboratory in 1924.

Keywords: geometrical optics; speed of light; reflection of light; elastic collision ball-wall; modified Michelson interferometer.

1. INTRODUCTION

The reflection of light as a mechanical phenomenon [1-3] considers the speed of light independent from its moving source and its reflection similar to a ball by a mirror in motion. This study continues with emission, propagation, and reflection of light as mechanical phenomena in inertial frames [4], observation of a star's orbit [5], a general consideration of light reflection [6,7], and here with the reflection of light applied to the Miller experiment [8,9].

The emission, propagation, and reflection of light in inertial frames [4] conclude that physics phenomena in an inertial frame can be studied in any other inertial frame considered at relative rest. Here, the Sun's frame at relative rest replaces the absolute frame for physics studies in Earth's inertial frame. Thus, the Sun is a fixed light source for Earth, and Earth may be considered an inertial frame in the Sun's frame at relative rest at the time of an experiment. The light from the Sun travels at the constant speed c in any direction in the Sun's frame at relative rest.

The reflection of light as a mechanical phenomenon applied to Michelson's interferometer with a particular geometry [1,2] predicts zero fringe shift, and to a geometry [3] close to that presented in the Michelson-Morley experiment [10] offers 0.40×10^{-4} fringe shift and greater for other geometries. Michelson's derivation predicts a 0.40 fringe shift.

This paper applies the theoretical derivation [1,2] and numerical calculation [3] to Miller's

experiments. Unlike the Tomaschek experiments [11], the fringe shifts in Miller's experiments are predictable.

The reflection of light as a mechanical phenomenon [1,2,5] based on the elastic collision of balls with a wall in motion at the limit when the mass of balls converges to zero offers the equation

$$c_{ra} = c_s + v_i + v_r. \quad (1)$$

In Eq. (1), c_{ra} is the speed of a reflected wavefront of a ray of light by a mirror in motion, c_s is the wavefront speed from the source or a mirror as a source, v_i is the mirror speed in the opposite direction of the incident wavefront from the source, and v_r is the mirror speed in the direction of the reflected wavefront. Here, these speeds are in the Sun's frame at relative rest. The mirror moves in one unique observable direction with speed v . However, regarding the light wavefront, as far as the collision effect is concerned, it has multiple directions of v_i and v_r at the moment of collision according to the mirror inclinations. Speeds v_i and v_r are projections of v in their corresponding directions.

Another form of Eq. (1) is

$$c_{ra} = c_s + v \cos a + v \cos b. \quad (2)$$

In Eq. (2), the speeds $v \cos a$ and $v \cos b$ replace v_i and v_r in Eq. (1), respectively. Angle a corresponds to the opposite direction of the incident wavefront, and angle b to the direction of the reflected wavefront. These angles are measured from the direction of velocity vector v , originating at the point of collision. The directions of v_i and v_r are outward from the point of collision.

Michelson [10] derives the fringe shift in the space filled with ether. Consequently, the speed of light from a source before and after reflection is the constant c . The study of light reflection as a mechanical phenomenon [1,2,5] occurs in a vacuum. Like a ball in an elastic collision with a wall, the wavefront speed changes after reflection by a moving mirror. Therefore, the difference between these two approaches is the reflection of light by a moving mirror.

2. INTERFEROMETER ON EARTH'S EQUATOR

2.1. General considerations

The following drawings illustrate a way to bring the light from the Sun to a modified Michelson interferometer. For simplicity, Earth's axis has no tilt.

Figure 1(a) illustrates Earth's equatorial circle, Earth's revolving orbit around the Sun, and the center of the Sun and Earth in the same plane. The North Pole is outward, and the South Pole is inward, perpendicular to the paper plane.

An observer in the Sun's frame at relative rest also perceives the physics phenomena as a local observer in Earth's inertial frame. The observer's location is on the North side of the Equator.

Figure 1(b) illustrates the Michelson interferometer at 6 am, as seen from the top side of Fig. 1(a). Mirrors M_1 , M_2 , M_3 , and beam splitter M belong to the instrument. Mirror M_3 replaces the instrument's source of light.

The cartesian frame $Oxyz$, fixed to the instrument, originates at point O of M_3 . Axis Ox is on the horizontal line, and axis Oz is perpendicular to Earth's local surface. Plane Oxy is parallel to Earth's local surface and perpendicular to the local Earth's radius. At 6 am, the revolving velocity v of Earth coincides with Oz .

The interferometer is in plane Oxy . It rotates counterclockwise around Oz with an angle f measured from Ox . The initial position of the instrument is when direction OM_1 coincides with Ox for $f = 0^\circ$, as shown in Fig. 1(b).

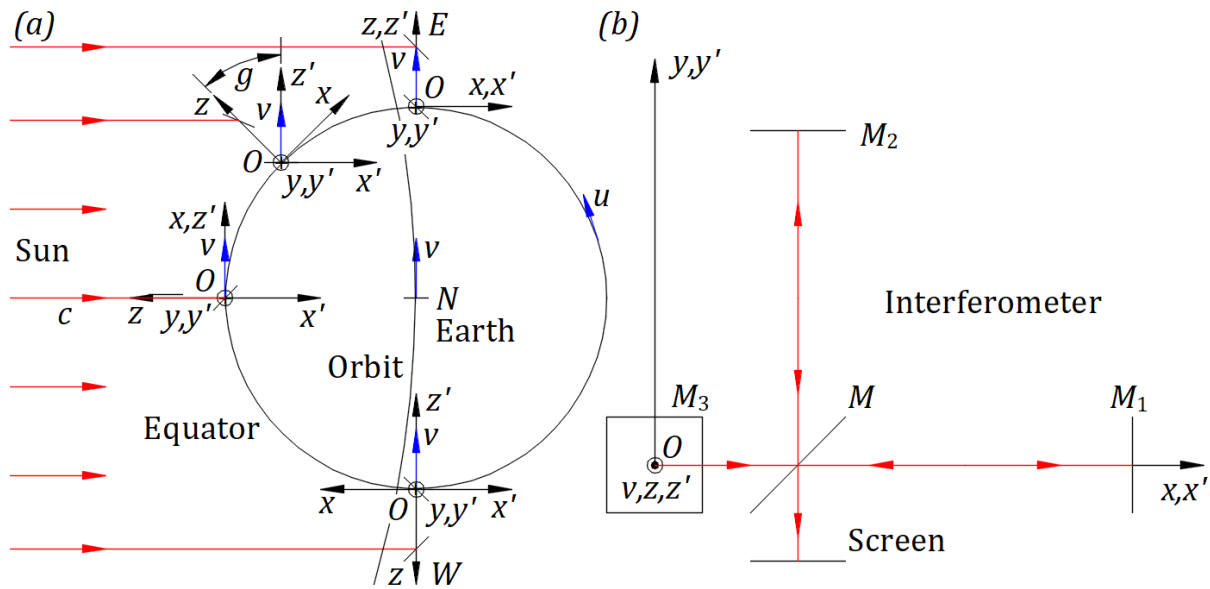


Figure 1. (a) Interferometer on Earth's Equator at 6 am, noon, 6 pm, and between 6 am and 6 pm. (b) Interferometer details.

In the Sun's frame at relative rest, a vector velocity v in the direction Oz' of the cartesian frame $Ox'y'z'$ is attached permanently to the origin O of $Oxyz$. Earth's spin changes the origin position O of $Oxyz$ and $Ox'y'z'$; different from $Oxyz$, $Ox'y'z'$ keeps its axes' directions fixed in the Sun's frame at relative rest.

The instrument on the Equator belongs to a local Meridian. The Equator's start position can be defined when: the local Meridian of the instrument is at 6 am, frames $Oxyz$ and $Ox'y'z'$ coincide, and the device is at the initial position, as illustrated in Fig. 1(b).

In the Sun's frame at relative rest, the center of the Sun, Earth's orbit, and the Equator's circle are always in the same plane. Planes Oxz and $Ox'z'$ belong to Equator's plane. Plane Oxy is parallel to Earth's local surface and perpendicular to Equator's plane. Axes Oy and Oy' are overlapping from 6 am to 6 pm.

Earth's spin changes the position of $Oxyz$. At the same time, in plane Oxz , axis Oz' rotates clockwise around Oy' , keeping the directions of $Ox'y'z'$ unchanged. Oz' with the vector velocity v at O makes the angle g measured from Oz .

Figure 1(a) indicates the position of the interferometer at 6 am, which is the Equator's start position, corresponding to $g = 0^\circ$. Earth's spin brings the interferometer to an angle g between 6 am and 6 pm, to $g = 90^\circ$ at noon, and $g = 180^\circ$ at 6 pm.

2.2. Interferometer on the Equator at 6 am, noon, and 6 pm

Figure 2(a) depicts the Equator's start position at 6 am for $g = 0^\circ$. Earth's spin brings the interferometer at noon, as illustrated in Fig. 2(b) for $g = 90^\circ$, at 6 pm, as presented in Fig. 2(c) for $g = 180^\circ$, and in general, at a time between 6 am and 6 pm, as shown in Fig. 3(a) for an angle g .

Point A belongs to mirror M_4 and to axis Oz . Mirror M_4 , axis Oz , mirror M_3 , and interferometer form a solid structure. Mirror M_4 rotates at the Equator around an axis through point A perpendicular to Oxz . At the North Pole around axis Oz . And between the Equator and the North Pole around both. M_4 stays fixed while the interferometer rotates 360° around axis Oz .

Considering that the Sun emits parallel rays of light in the direction from the Sun's center toward Earth's center, only these rays are reflected by M_4 in the opposite direction to Oz toward M_3 . The incident rays from the Sun are perpendicular to v at any location on Earth.

In Fig. 2(a), point A of M_4 reflects the ray of light toward O with the speed c_{ra} given by Eq. (2), $c_{ra} = c_s + v \cos a + v \cos b = c + v \cos 90^\circ + v \cos 180^\circ = c - v$.

The ray reflected at O along Ox and OM_1 for $f = 0^\circ$ has the speed $c_{f=0^\circ} = c_s + v \cos a + v \cos b$. With $c_s = c_{ra}$, $c_{f=0^\circ} = (c - v) + v \cos 0^\circ + v \cos 90^\circ = c$.

The projection of v on Oz is $v_z = v$. The rays reflected by M_3 drift transversal opposite to velocity v_z .

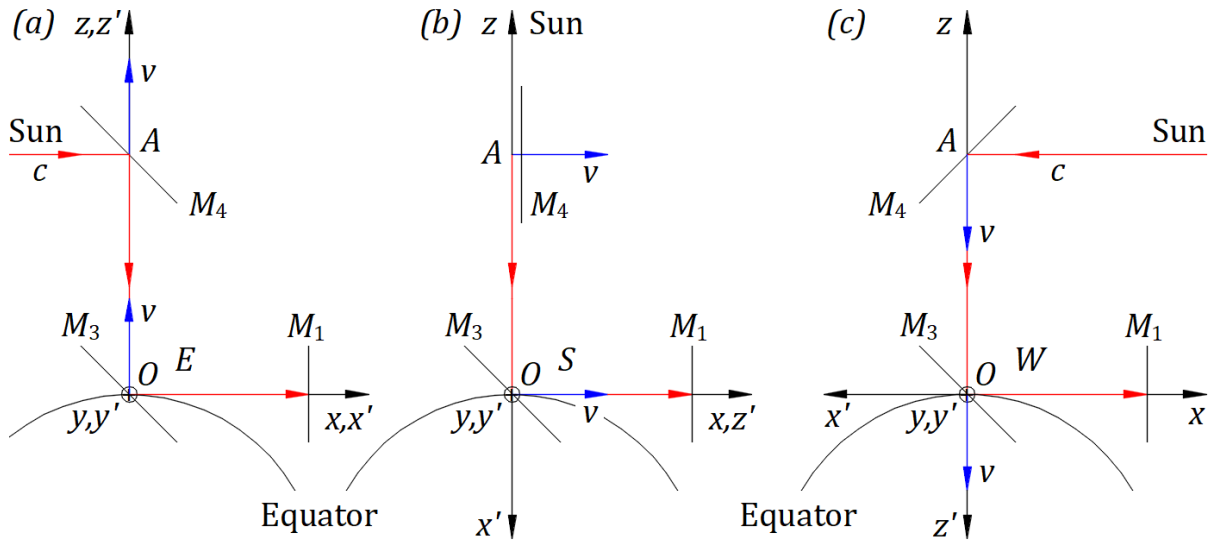


Figure 2. Interferometer on the Equator: (a) at 6 am, (b) at noon, and (c) at 6 pm.

In Fig. 2(b), the light from the Sun travels perpendicular to Ox ; therefore, no need for mirror M_4 . At this position, M_4 rotates 180° around Oz to continue reflecting rays for $90^\circ < g \leq 180^\circ$.

The ray reflected at O along Ox and OM_1 for $f = 0^\circ$ has, according to Eq. (2), the speed $c_{f=0^\circ} = c_s + v \cos a + v \cos b = c + v \cos 90^\circ + v \cos 0^\circ = c + v$.

The projection of v on Oz is zero. Thus, there is no transversal drift on rays reflected at M_3 .

Figure 2(c) shows the device at 6 pm. Point A of M_4 reflects the ray of light toward O with the speed c_{ra} given by Eq. (2), $c_{ra} = c_s + v \cos a + v \cos b = c + v \cos 90^\circ + v \cos 0^\circ = c + v$.

The ray reflected at O along Ox and OM_1 for $f = 0^\circ$ has the speed $c_{f=0^\circ} = c_s + v \cos a + v \cos b = c_{ra} + v \cos 180^\circ + v \cos 90^\circ = (c + v) - v = c$.

The projection of v on Oz is $v_z = -v$. The rays reflected by M_3 drift transversal opposite to velocity v_z .

2.3. Interferometer on the Equator at an angle g

Figure 3(a) presents the instrument between 6 am and 6 pm when Oz' makes an angle g measured from Oz . To reflect the rays in the direction AO , M_4 rotates around the axis through point A and perpendicular to Oxz . Angle g has an opposite direction to Earth's spin.

From 6 am to 6 pm for $0^\circ \leq g \leq 180^\circ$, projection of v on Oz is the transversal speed of the instrument in the Sun's frame at relative rest

$$v_z = v \cos g. \quad (3)$$

Projection of v on Ox is the longitudinal speed of the instrument in the Sun's frame at relative rest $v_x = v \cos(90^\circ - g)$, then

$$v_x = v \sin g. \quad (4)$$

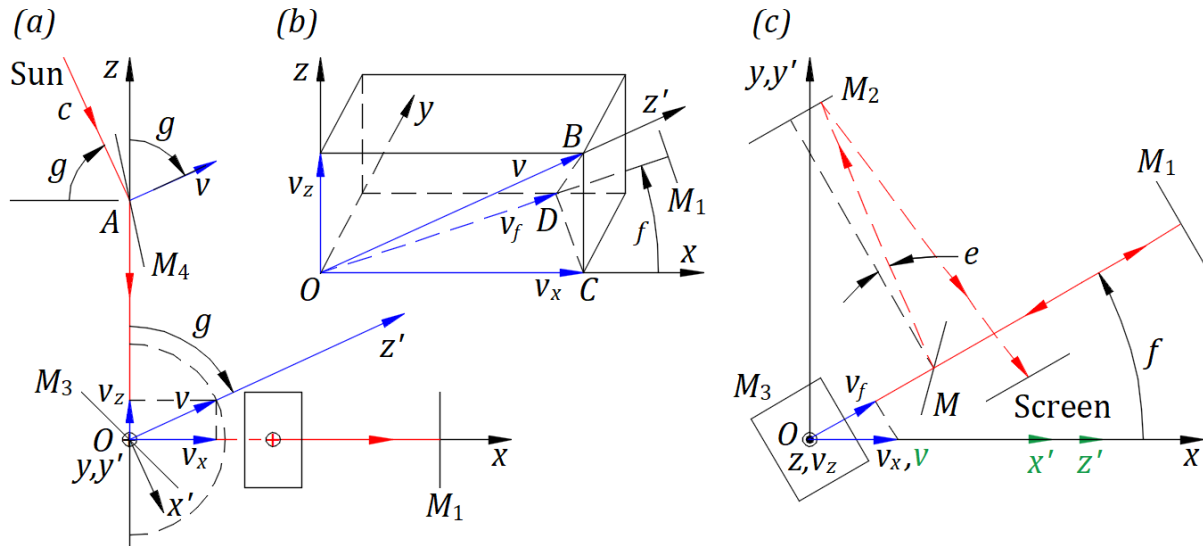


Figure 3. (a) Interferometer at an angle g . (b) Three-dimensional detail of mechanical velocities at point O . (c) Interferometer at an angle f from Ox illustrated in plane Oxy .

Figure 3(b) is a detail at point O in a three-dimensional view when the instrument is at an angle f from Ox . OBC and BCD planes and their intersection along BC are perpendicular to Oxy , and BD is perpendicular to OM_1 . Therefore, OD is perpendicular to plane BCD , and CD is perpendicular to OD . Thus, the projections of v and v_x on OM_1 are identical to $OD = v_f$; with v_x from Eq. (4),

$$v_f = v_x \cos f. \quad (5)$$

Figure 3(c) illustrates the top side view of Fig. 3(a) with the interferometer rotated by an angle f from Ox . For the geometry presented in Ref. [3], reflected rays by beam splitter M travel as illustrated at an angle e from the perpendicular line to M_2 . Ox' , Oz' , and v in green indicate that they are not in plane Oxy .

Point A of M_4 reflects the ray of light toward O with the speed $c_{ra} = c_s + v \cos a + v \cos b = c + v \cos 90^\circ + v \cos(180^\circ + g)$ that gives the equation

$$c_{ra} = c - v \cos g. \quad (6)$$

The ray from A reflected at O along Ox , employing Eq. (2), has the speed $c_{f=0^\circ} = c_{ra} + v \cos a + v \cos b$. With c_{ra} from Eq. (6) and v_x from Eq. (4), $c_{f=0^\circ} = (c - v \cos g) + v \cos g + v \sin g$ yields the equation

$$c_{f=0^\circ} = c + v_x. \quad (7)$$

The reflected speed of light at O along OM_1 at an angle f is $c_f = c_{ra} + v \cos a + v \cos b = (c - v \cos g) + v \cos g + v_x \cos f$, therefore,

$$c_f = c + v_x \cos f. \quad (8)$$

3. INTERFEROMETER ON THE NORTH POLE

The solid structure, illustrated in Fig. 2(a), brought from the Equator at 6 am along the local Meridian at the North Pole, looks like in Fig. 4(a). From the Equator to the North Pole, the frame $Oxyz$ rotates 90° in the Sun's frame at relative rest. In plane Oyz , Oz' rotates 90° around Ox' from Oz to Oy ; after rotation, Oz' has the same direction as Oy . Planes Oxy and $Ox'z'$ coincide and are parallel to Equator's plane. Axis Oy' is perpendicular to Equator's plane.

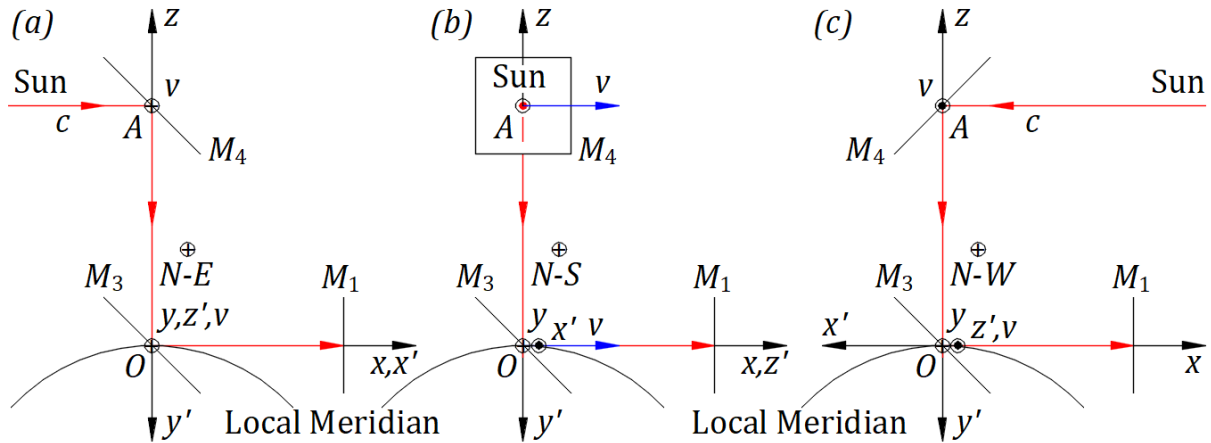


Figure 4. Interferometer on the North Pole: (a) at 6 am, (b) at noon, and (c) at 6 pm

Earth's spin rotates $Oxyz$ in the Sun's frame at relative rest. In plane Oxy , Oz' rotates around fixed Oy' from Oy at 6 am at angle $g = 0^\circ$, as illustrated in Fig. 4(a), to Ox at noon at angle $g = 90^\circ$, as in Fig. 4(b), and to $-Oy$ at 6 pm at angle $g = 180^\circ$, as in Fig. 4(c). At the North Pole, mirror M_4 rotates only around Oz .

4. INTERFEROMETER ON A LATITUDE

The right side view of Fig. 2(a), ignoring M_1 , is as in Fig. 5(a). Moving the solid structure from the Equator toward the North Pole, $Oxyz$ rotates in the Sun's frame at relative rest. Velocity v with its axis Oz' rotates in plane Oyz around Ox' with angle h measured from axis Oz , as visualized in Fig. 5(b). For $h = 0^\circ$, the interferometer is at the Equator, and for $h = 90^\circ$ at the North Pole. In the rotation on a Meridian, from the Equator to the North Pole, Mirror M_4 stays fixed.

In Fig. 5(b), we can define the Latitude's start position at the intersection of the local Meridian with the local Latitude at 6 am. Oz' is marked with index o for angle $g = 0^\circ$, Oz'_o , and is in plane Oyz making an angle h measured from Oz .

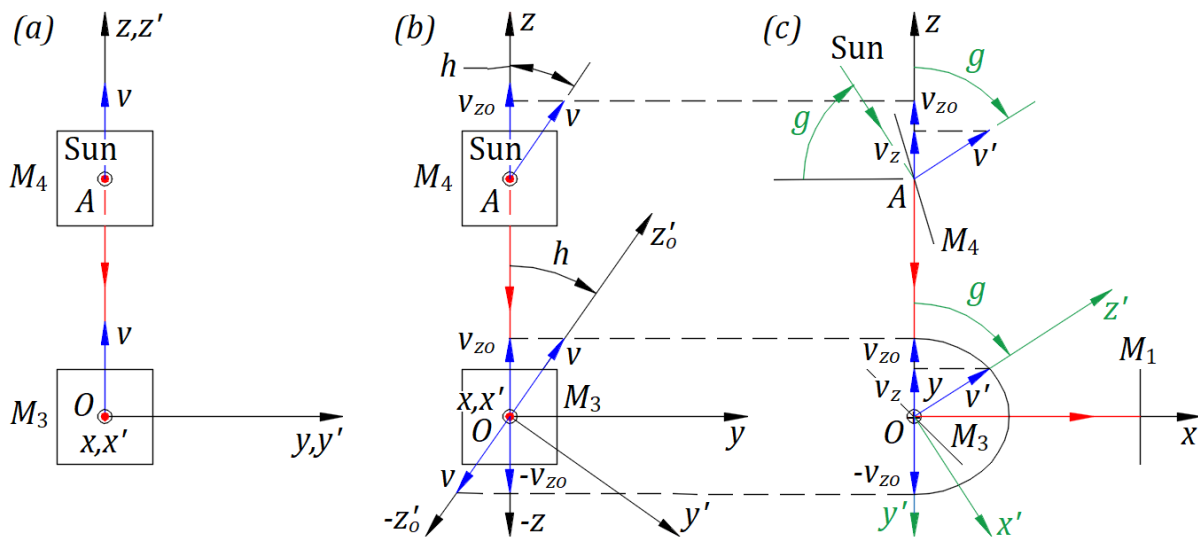


Figure 5. (a) Interferometer on the Equator at 6 am. Interferometer on a Latitude: (b) at angle h , and (c) left side view of Fig. 5(b).

Plane $Ox'z'$ is parallel, and axis Oy' is perpendicular to Equator's plane here and at any location on Earth. Plane Oxy is parallel, and the axis Oz is perpendicular to Earth's local surface as on any place on Earth. Oxz and $Ox'z'$ are perpendicular to plane Oyz and intersect along Ox .

Earth's spin rotates the frame $Oxyz$ on the Latitude from 6 am to 6 pm. At the same time, velocity v with its axis Oz' rotates around fixed axis Oy' from Oz'_o at 6 am for angle $g = 0^\circ$ to Ox at noon for $g = 90^\circ$ and to $-Oz'_o$ at 6 pm for $g = 180^\circ$. Thus, on a Meridian, angle g is identical when the instrument is on different Latitudes to that at the Equator. On a Latitude, mirror M_4 rotates around both axes to capture only the parallel rays from the Sun.

The view from the opposite direction of Oy' shows vector v with its axis Oz' rotating from 6 am to 6 pm on a semicircle with origin at O and radius v . The semicircle is in plane $Ox'z'$. Any angle h yields an identical image. The semicircle is identical to that in Fig. 3(a), illustrated in a dashed line in plane Oxz .

The view from the opposite direction of Oy sees the semicircle projection of the vector v as a semi-ellipse in plane Oxz , as illustrated in Fig. 5(c). The projection points of this semi-ellipse on Oz represent the speeds v_z for angles g .

Figure 5(c) is the left side view of Fig. 5(b) for an angle g measured from Oz'_0 . The projection of the velocity v that belongs to Oz' on plane Oxz is v' . Ox' , Oy' , and Oz' axes are depicted in green to indicate that they are not in plane Oxz ; Ox' is in the front, and Oy' and Oz' are in the back of plane Oxz .

Planes Oxz and $Ox'z'$ intersect along Ox . Ox' coincides with Ox only at $g = 0^\circ$. Axis Oz' rotates in the back of plane Oxz from Oz'_0 at the Latitude's start position when it is behind Oz for $g = 0^\circ$ to plane Oxz coinciding with Ox for $g = 90^\circ$. Then Oz' rotates in front of plane Oxz to $-Oz'_0$ for $g = 180^\circ$, above $-Oz$. Ox' rotates in front of plane Oxz from Ox for $g = 0^\circ$ to above $-Oz$ for $g = 90^\circ$, then to $-Ox$ for $g = 180^\circ$.

Figure 6(a) offers a three-dimensional visualization of the mechanical velocities at point O of Fig. 5(c). Axis Oz'_0 is in plane Oyz . Rectangular $ODEH$ belongs to Oxz , $ODCG$ to Oxy , and $OGFH$ to Oyz . The speed v is along axis Oz' . Index i for M_{1i} indicates that mirror M_1 location corresponds to angles i defined below. Velocities v and $v_{z'_0}$ belong to rectangular $ODBF$ of the plane in red; v_x and v_i to plane Oxy .

The projection of v on Oz at the Latitude's start position offers the equation

$$v_{zo} = v \cos h. \tag{9}$$

The projection of v on Oz'_0 is $OF = v_{z'_0}$, therefore,

$$v_{z'_0} = v \cos g. \tag{10}$$

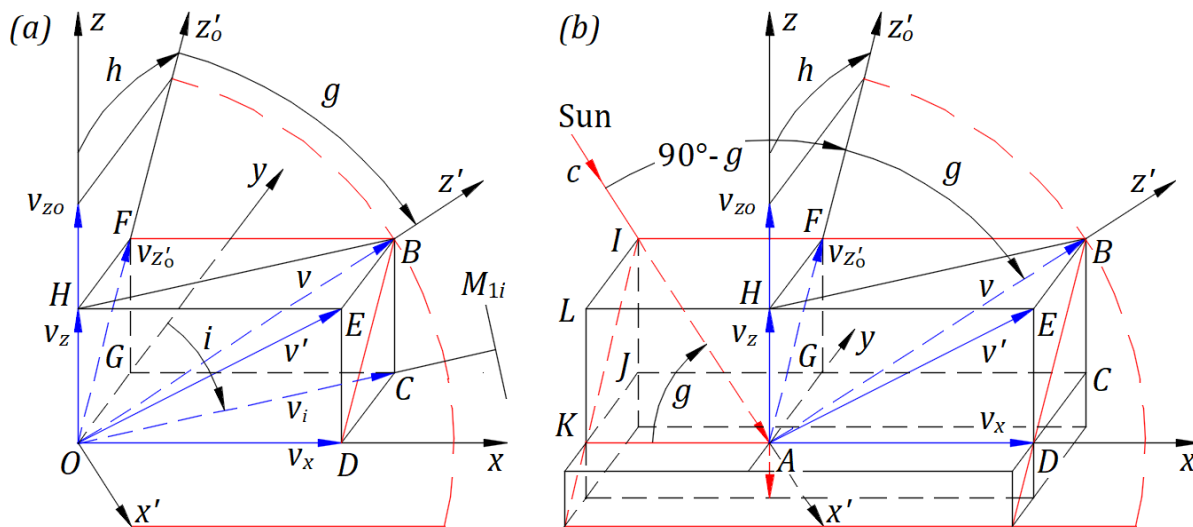


Figure 6. Mechanical velocities of Fig. 5(c): (a) at point O and (b) at point A .

The projection of $v_{z'_0}$ on Oz , $v_z = v_{z'_0} \cos h$, is also the projection of v on Oz . Employing Eq. (10),

$$v_z = v \cos h \cos g. \quad (11)$$

v_z is the transversal speed of the instrument in the Sun's frame at relative rest.

Ox belongs to $Ox'z'$ as well. The projection of v on Ox is $v_x = v \cos(90^\circ - g)$, therefore,

$$v_x = v \sin g. \quad (12)$$

$BC = OH = v_z$. From triangle OBC , the longitudinal velocity of the instrument in the Sun's frame at relative rest has the magnitude of $v_i = \sqrt{v^2 - v_z^2}$ that with v_z from Eq. (11) yields the equation

$$v_i = v\sqrt{1 - (\cos h \cos g)^2}. \quad (13)$$

In triangle OCG , $\sin i = GC/v_i = v_x/v_i$, then

$$i = \sin^{-1}(v_x/v_i). \quad (14)$$

Angle i indicates the interferometer's initial position direction OM_{1i} when OM_1 and v_i directions coincide.

Figure 6(b) offers a three-dimensional visualization of the mechanical velocities at point A of Fig. 5(c). At A , we can attach the same frame as at O , $Axyz$, and $Ax'y'z'$. Axis Az'_0 is in plane Ayz . Velocities v and $v_{z'_0}$ belong to rectangular $BDKI$ of plane $Ax'z'$, which contains red lines. The ray from the Sun travels in this plane along the line IA . Point A of M_4 reflects it towards O . M_4 must be adjusted with both axes to reflect the incident ray along axis Ax' from I to A towards O .

The ray of light reflected at A toward O has the speed $c_{ra} = c_s + v \cos a + v \cos b = c + v \cos 90^\circ - v_z$ that gives the equation

$$c_{ra} = c - v_z. \quad (15)$$

From Fig. 6(a), the speed of light reflected in the direction M_{1i} for angle i , $c_i = c_{ra} + v \cos a + v \cos b = (c - v_z) + v_z + v_i$, offers the equation

$$c_i = c + v_i. \quad (16)$$

Equation (16) corresponds to Eq. (7) when the interferometer is on the Equator.

For the same reason as in Fig. 3(b), the projections of v and v_i along OM_1 are identical for any angle f measured from M_{1i} . The speed of light reflected at O in the direction of OM_1 for an angle f measured from M_{1i} is $c_{if} = c_{ra} + v \cos a + v \cos b = (c - v_z) + v_z + v_i \cos f$ that yield the equation

$$c_{if} = c + v_i \cos f. \quad (17)$$

Equation (17) corresponds to Eq. (8) when the interferometer is on the Equator.

5. NUMERICAL CALCULATION OF THE FRINGE SHIFT

For the length $L = 32$ m of the interferometer's arms, Miller expected a 1.12 fringe shift based on Michelson's derivation [10] and observed, at Mount Wilson, 0.08 in 1921 and 0.088 in 1925 [8,9]. The observations taken in the laboratory at Cleveland 1924, with sunlight and laboratory sources, show a null result of experiments. The above discrepancy in experimental results requires a theory to support it or a reevaluation of Miller's experiments.

The velocity v is the moving velocity of the instrument in the Sun's frame at relative rest. The device has the longitudinal velocity v_x at the Equator and v_i on a Meridian parallel to and the transversal velocity v_z perpendicular to plane Oxy . To correctly calculate the fringe shift within the interferometer, we have to consider both velocities, but there is no such theoretical derivation.

In the following derivation, we assume that the fringe shift is not affected by the transversal speed v_z , and we calculate the fringe shift for the four positions offered by Ref. [3].

The numerical calculation can be performed on a spreadsheet according to the theoretical derivation of Ref. [3], starting with the set of speeds c_{11} , c_{12} , c_{13} , c_{21} , and c_{22} , followed by the times the light travels its paths and their differences, and finally, the fringe shift, for each of the four positions at angle $a = 0^\circ$, 90° , 180° , and 270° .

The initial position of the interferometer for $f = 0^\circ$ corresponds to the $a = 180^\circ$ position in Ref. [3] because between the two selected initial positions, there is a difference of 180° . Thus, for $f = 0^\circ$, 90° , 180° , and 270° positions correspond to $a = 180^\circ$, 270° , 0° , and 90° positions in Ref. [3].

The speed c_{if} from Eq. (17) replaces the speed c correspondingly in the sets of speeds c_{11} , c_{12} , c_{13} , c_{21} , and c_{22} in the four positions as defined in Ref. [3]. The numerical magnitude of speed v_i from Eq. (13) replaces speed v in all four positions of Ref. [3], including the above sets of speeds.

In Ref. [3], rays along the screen interfere because their speeds, c_{13} and c_{22} , are equal. Ref. [3] derives the difference between the two light paths in the number of wavelengths $N_{1,2,3,4} = c\Delta t_{1,2,3,4}/\lambda$, where $\Delta t_{1,2,3,4} = t_2 - t_1$ for each of the four positions. $\Delta t_{1,2,3,4}$ is the difference in the time the two rays travel their paths with the same or different speeds. c is the constant 3×10^8 m/s and λ the wavelength of light for constant c .

If the speed of the two interfering rays increases or decreases, their wavelengths increase or decrease directly proportional. Therefore, the ratio speed/wavelength is a constant for any of their corresponding speeds/wavelengths. Therefore, $N_{1,2,3,4}$ are not affected by the speed magnitude of rays that interfere along the way to the screen. Thus, no need to change the formula $N = c\Delta t_{12}/\lambda$. The speed of the interfering rays affects the spread of the fringes that is unobservable.

For any location on Earth, the numerical calculation of the fringe shift, for $L = 32$ m, predicts unobservable fringe shifts in the 10^{-8} range. For $L = 10^8$ m, the fringe shift is in the range of 10^{-1} . The rays reflected by M_4 coming from different points of the Sun, or v corresponding to different altitudes, or

magnitudes of angle e greater than aberration angle do not change the result of the fringe shifts.

In Ref. [3], different from this article, the source of light is a part of the interferometer belonging to Earth's inertial frame. For $L = 11$ m, the fringe shift is 0.4×10^{-4} ; for $L = 32$ m, is 1.16×10^{-4} . According to emission, propagation, and reflection of light as mechanical phenomena in inertial frames [4], the fringe shift in the Michelson interferometer is zero.

6. CONCLUSIONS

With the assumption that the transversal velocity of the interferometer v_z does not affect the fringe shift, Michelson derivation does not agree with Miller's experiments at Mount Wilson in 1921 and 1925 and those at Cleveland laboratory in 1924. The derivation based on the reflection of light as a mechanical phenomenon does not agree with Miller's experiments at Mount Wilson but agrees with experiments at Cleveland laboratory with sunlight and laboratory sources.

When the local meridian is at noon, from the Equator to the North Pole, there is no transversal speed for the instrument, and the numerical calculation yields zero fringe shift. Miller observed fringe shifts at Mount Wilson for these positions as well. Therefore, a derivation considering the transversal speed should not affect the fringe shift for these positions and is not likely for any position of the instrument on Earth.

For any angle f , the speed of light $c_{if} = c + v_i \cos f$, and the longitudinal speed of the interferometer is $v_i \cos f$. Thus, the speed of light within the interferometer is c , which could explain why the fringe shift is zero or undetectable.

The Tomaschek experiment [11] may display a fringe shift if the star's velocity in the Universe is different from that of the Sun. The light from a star arrives on Earth, no matter the distance from the star to the Sun, with two components: the emitted velocity c and the star's velocity [4,5]. The fringe shift depends on the difference of star and Sun velocities. Experiments consist of trials and observations with different stars without any expectations. Nevertheless, the theoretical derivation is more complex, even if we know the star's velocity to the Sun.

However, regardless of the outcome of a complete theoretical derivation, the contradictory results observed at Mount Wilson and the Cleveland laboratory leave this subject open to theoretical and experimental challenges.

Ref. [3], in which the source belongs to the interferometer, offers zero fringe shift for $e = 0$ rad, 0.40×10^{-4} for aberration angle $e = 0.0001$ rad, and greater than 0.40×10^{-4} for an angle e beyond the aberration angle. We chose a geometry for theoretical derivation and calculation of the fringe shift, but an experiment yields a fringe shift according to an unknown geometry. Since different magnitudes of angle e can explain different fringe shifts for the same interferometer, the author expected to explain Miller's observations at Mount Wilson and Cleveland Laboratory.

References

1. Filipescu, F. D. Reflection of Light as a Mechanical Phenomenon Applied to a Particular Michelson Interferometer. *Preprints* **2020**, 2020090032 (doi: 10.20944/preprints202009.0032.v1).
2. Filipescu, F. D. Opposing hypotheses of the reflection of light applied to the Michelson interferometer with a particular geometry. *Phys. Essays*. **2021**, 34, 3, 268-273.

3. Filipescu, F. D. Opposing hypotheses of the reflection of light applied to the Michelson interferometer. *Phys. Essays*. **2021**, 34, 3, 389-396.
4. Filipescu, F. D. Emission, propagation, and reflection of light as mechanical phenomena in inertial frames. *Phys. Essays*. **2021**, 34 587-590.
5. Filipescu, F. D. Observation of a star's orbit based on the emission and propagation of light as mechanical phenomena. *Phys. Essays*. **2022**, 35, 2, 111-114.
6. Filipescu, F. D. Emission, Propagation, and Reflection of Light as Mechanical Phenomena. *Preprints* **2022**, 2022040061 (doi: 10.20944/preprints202204.0061.v2).
7. Filipescu, F. D. Emission, propagation, and reflection of light as mechanical phenomena: General considerations. *Phys. Essays*. **2022**, 35, 3, 266-269.
8. Miller, D. C. Ether-Drift Experiments at Mount Wilson. *Proc. Natl. Acad. Sci. U. S. A.* **1925**, 11, 6, 306-314.
9. Miller, D. C. The Ether-Drift Experiment and the Determination of the Absolute Motion of the Earth. *Reviews of Modern Physics*. **1933**, 5 (3): 203–242.
10. Michelson, A. A.; Morley, E. W. On the relative motion of the earth and the luminiferous ether. *Am. J. Sci.* **1887**, 34, 203, 333–345.
11. Tomaschek, R. Über das Verhalten des Lichtes außerirdischer Lichtquellen. *Ann. Phys.* **1924**, 378, 1-2, 105-126.